Journal of Ginseng Research 49 (2025) 80–91

Contents lists available at ScienceDirect

Journal of Ginseng Research

journal homepage: www.sciencedirect.com/journal/journal-of-ginseng-research

Research Article

Ginsenoside Rg1 improves hypoxia-induced pulmonary vascular endothelial dysfunction through TXNIP/NLRP3 pathway-modulated mitophagy

Ru Zhang, Meili Lu, Chenyang Ran, Linchao Niu, Qi Qi, Hongxin Wang *

The Key Laboratory of Cardiovascular and Cerebrovascular Drug Research of Liaoning Province, Jinzhou Medical University, Jinzhou, China

ARTICLE INFO

Keywords:
Ginsenoside Rg1
Vascular endothelial dysfunction
Pulmonary arterial hypertension
TXNIP
NLRP3

ABSTRACT

Background: Vascular endothelial dysfunction (VED) is one of the main pathogenic events in pulmonary arterial hypertension (PAH). Previous studies have demonstrated that the ginsenoside Rg1 (Rg1) can ameliorate PAH, but the mechanism by which Rg1 affects pulmonary VED in hypoxia-induced PAH remains unclear.

Methods: Network pharmacology, molecular docking and other experiments were used to explore the mechanisms by which Rg1 affects PAH. A PAH mouse model was established via hypoxia combined with the vascular endothelial growth factor (VEGFR) inhibitor su5416 (SuHx), and a cell model was established via hypoxia. The functions of Rg1 in VED, oxidative stress, inflammation, mitophagy, and TXNIP and NLRP3 expression were examined.

Results: In hypoxia-induced VED, progressive exacerbation of oxidative stress, inflammation, and mitophagy were observed, and were associated with elevated TXNIP and NLRP3 expression in vivo and in vitro. Rg1 improved hypoxia-induced impaired endothelium-dependent vasodilation and increased nitric oxide (NO) and endothelial NO synthase (eNOS) expression. Rg1, SRI37330 (a TXNIP inhibitor), MCC950 (an NLRP3 inhibitor), and Liensinine (a mitophagy inhibitor) attenuated oxidative stress, inflammation, and mitophagy by reducing the expression of TXNIP and NLRP3 in mice and cells. Furthermore, the combination of SB203580 (a mitophagy agonist) with Rg1 disrupted the protective effect of Rg1 on hypoxia-induced pulmonary artery and human pulmonary artery endothelial cells (HPAECs).

Conclusion: Rg1 improves hypoxia-induced pulmonary vascular endothelial dysfunction through TXNIP/NLRP3 pathway-modulated oxidative stress, inflammation and mitophagy.

1. Introduction

This study aimed to elucidate the therapeutic mechanism of ginsenoside Rg1 (Rg1) on pulmonary arterial hypertension (PAH) using a network pharmacology approach. Topology analysis aids researchers in understanding how drugs affect biological systems. Cluster analysis, assists in the discovery of novel drug candidates. Gene Ontology (GO) analysis and Kyoto Encyclopedia of Genes and Genomes (KEGG) analysis were used to reveal the functions and interaction networks of biomolecules. Finally, molecular docking, provides precise binding site information for drug design.

PAH is a disease characterized by pulmonary vascular contraction, microvascular obstruction, and arterial removal, which may lead to premature death [1–3], and its development is dependent on vascular endothelial dysfunction (VED) [4]. The main features of VED are an imbalance between blood vessels and blood vessel contraction factors, excess production of inflammatory medium and overproduction of vascular smooth muscle cells.

Oxidative stress and inflammation are important elements of VED, and there is a close interaction between them. Excessive reactive oxygen species (ROS) and/or antioxidant deficiency cause lipid oxidation to stimulate cell damage, thereby impairing their function. This stress also reduces the biological usage of nitric oxide (NO), and impairs endothelium-dependent vasodilatory function. Inflammation is characterized can activate endothelial cells and enhance inflammatory reactions. Activation of inflammation further amplifies oxidative stress, creating a vicious cycle that exacerbates VED; therefore, therapeutic strategies targeting oxidative stress and inflammation are essential for

* Corresponding author. Department of Pharmacology, Jinzhou Medical University, No.40.Section 3, Songpo Road, Jinzhou City, Liaoning, 121001, China.
E-mail address: hongxinwang@jzmu.edu.cn (H. Wang).

https://doi.org/10.1016/j.jgr.2024.10.002
Received 12 June 2024; Received in revised form 15 October 2024; Accepted 23 October 2024
Available online 24 October 2024

ameliorating VED [5–7].

Mitophagy is a selective macroautophagy process that removes damage and dysfunction. In the case of oxidative stress, DNA damage, or other damage, mitochondria are damaged by energy metabolism and increased ROS. Failure to remove damaged mitochondria in a timely manner can lead to VED through the release of proinflammatory factors. Mitophagy maintains the stability of energy metabolism by reducing the production of ROS, protecting the function of endothelial cells and preventing oxidative stress. This protective effect is important for maintaining the structure and function of the vascular endothelium and preventing the occurrence and pathogenesis of VED [8–10]. Mitophagy also regulates inflammation and helps prevent endothelial dysfunction. Therefore, regulating mitophagy may be an effective method for relieving and treating VED.

Thioredoxin interacting protein (TXNIP), a protein closely related to oxidative stress, suppresses thioredoxin by combining with the important antioxidant sulfur oxygen reduction protein (TRX) and oxidizing cells to regulate the reduction and inflammatory reactions. An increase in TXNIP levels is related to oxidative stress and inflammatory reactions in many diseases, promoting mitophagy, but mitophagy is an important process of stable energy metabolism in cells [11,12]. NLRP3 is a nod-like receptor (NLR) family member that activates caspase-1, and promotes the maturation and secretion of the inflammatory cytokines IL-1β and IL18, which play important roles in disease pathogenesis. Activation of TXNIP induces the formation of NLRP3 inflammatory vesicles, triggering mitochondrial stress-induced apoptosis and the release of inflammatory factors. Activation of NLRP3 is also associated with mitochondrial dysfunction and has the potential to further activate mitophagy [13,14]. In the TXNIP/NLRP3 pathway, TXNIP may regulate NLRP3 activation by affecting mitochondrial function and promoting mitophagy. Activation of the NLRP3 inflammasome may exacerbate mitochondrial damage, thus creating a positive feedback loop leading to increased mitophagy and inflammation. In summary, the intricate interplay between the TXNIP/NLRP3 pathway and mitophagy is crucial for controlling inflammatory responses in cells and preserving intracellular homeostasis.

Rg1, one of the principal active components of ginseng, which is characterized by antiapoptotic, antioxidative, and anti-inflammatory effects [15–17]. In recent years, Rg1 has been shown to protect against low-salt stress-induced endothelial cell damage and high glucose-induced endothelial barrier dysfunction [18,19]. Previous research from our laboratory has shown that Rg1 improves VED induced by chronic intermittent hypoxia (CIH) and high glucose [20,21]. Recently, it has been demonstrated that many related references linking Rg1 and mitophagy in many different diseases [22–24]. Therefore, it is important to further study the protective effects of Rg1 on PAH-related VED and the underlying mechanisms. The purpose of this study was to determine whether Rg1 regulates oxidative stress, inflammation, and mitophagy through the TXNIP/NLRP3 pathway and improves hypoxia-induced VED.

2. Materials and methods

2.1. Network pharmacology

The SEA (https://sea.bkslab.org/), ECTM (http://www.tcmip.cn/ETCM/) and SwissTarget (https://www.swisstargetprediction.ch/) databases were used to screen the corresponding targets of Rg1. The PAH and pulmonary VED targets were obtained from the OMIM (https://www.omim.org/), DisGeNET (https://www.disgenet.org/) and the GeneCards database (https://www.genecards.org/). A Venn diagram was used to identify the targets of bioactive components associated with PAH and Rg1. The shared targets were uploaded to the STRING database (https://string-db.org/) for protein–protein interaction (PPI) analysis. Cytoscape 3.6.1 was used to visualize the common targets. Metascape (http://metascape.org/) was used for GO enrichment and KEGG analysis, and visualization was performed using bioinformatics (http://www.bioinformatics.com.cn/).

2.2. Molecular docking

AutoDock Vina 4.2 was used for molecular docking. The PubChem database (https://pubchem.ncbi.nlm.nih.gov/) was used to download the 2D structure of Rg1. The 2D structure was processed and converted to 3D by Chem3D 22.0.0 software. The 3D structures of macromolecular receptors were downloaded from the Protein Data Bank database (https://www.rcsb.org/) and visualized in PyMOL 3.8.

2.3. Animal experiments

Animal surgeries were approved by the Ethics Committee for Animal Experiments of Jinzhou Medical University. Sixty male C57BL/6 mice (Liaoning Changsheng Biotechnology) were randomly divided into six groups: control group (Con), hypoxia combined with su5416 (vascular endothelial growth factor (VEGFR) inhibitor su5416; GLPBIO) group (SuHx), SuHx + Rg1 low-dose group (Rg1 (Nanjing Jingzhu Biotechnology, purity >98 %) L, 5 mg/kg/d), Rg1 medium-dose group (Rg1M, 10 mg/kg/d), Rg1 high-dose group (Rg1H, 20 mg/kg/d) and positive control group (Sildenafil, Pfizer, 100 mg/kg/d). Mice in the SuHx group and each dosing group were placed in an automatically controlled hypoxia chamber and exposed to 20 hypoxia events/hour (21 % O_2 for 90 s and 10 % O_2 for 90 s) per day for a duration of 8 h for 4 weeks. The control mice were placed in the same normal oxygen environment. During the period of hypoxia, mice in the model group and each dosing group were given subcutaneous injections of Su5416 (20 mg/kg) twice weekly, and the dosing group was gavaged daily with the appropriate dose.

2.4. Cell culture

Human pulmonary arterial endothelial cells (HPAECs, BLUEFBIO) were cultured in an incubator at 37 °C (5 % CO_2) in 10 % DMEM (Gibco, Thermo Fisher) containing bovine fetal serum. The cells were incubated with Rg1 (20 μM), SRI37330 (1 μM, a TXNIP inhibitor; MCE), MCC950 (2 μM, an NLRP3 inhibitor; MCE), Sildenafil (5 μM), SB203580 (5 μM, MCE), and Liensinine (20 μM, MCE) for 12 h. The treated HPAECs were then exposed to 37 °C, 1 % O_2 for 25 min, and 20 % O_2 for 5 min for 24 h.

2.5. Hemodynamic measurements

After the mice were anesthetized (1 % sodium pentobarbital; Sigma Aldrich), tha sterile catheter was inserted into the jugular vein and connected to a pressure transducer, and the right ventricular systolic pressure (RVSP) and mean pulmonary artery pressure (mPAP) were measured.

2.6. Hemodynamic measurements

Using a high-resolution Sigma VET ultrasound system, evaluated right heart function in spontaneously breathing mice. The mice chest was depilated and applied with ultrasound coupler, and room temperature was controlled at 25 °C to prevent hypothermia.

2.7. HE staining

Mouse pulmonary arteries were fixed, dehydrated, cleared, wax immersed, and embedded into sections. After fixation, tissues were dehydrated through a graded series of ethanol, cleared in xylene, and embedded in paraffin. Sections of 4–5 μm thickness were cut, deparaffinized, rehydrated, and stained with hematoxylin and eosin (H&E).

2.8. Vascular reactivity

The vessels were cut into circular segments (approximately 2–3 mm) and attached to another wire dystonia chamber. Each chamber was filled with saline containing 5 % CO_2+95 % O_2 (37 °C). The pulmonary arteries of blank control mice were cultured with Rg1 (10, 20 or 40 μM), SRI37330 (1 μM), MCC950 (2 μM), Sildenafil (5 μM), Rg1 (20 μM) + SB203580 (5 μM) or Liensinine (20 μM) for 4 h and then subjected to hypoxia for 1 h (5 % CO_2+95 % N_2 was replaced with hypoxia for 30 min, and a low oxygen environment was created). Induced vasoconstriction by PE (phenylephrine, 10^{-5} M; Sigma Aldrich) and Ach (acetylcholine, 10^{-9}–10^{-4} M; Sigma Aldrich) accumulated to induce dilation, and the contraction response of the vascular ring was recorded to construct a dose–response curve.

2.9. Measurement of NO levels and NO imaging

Pulmonary arteries were removed from the mice, the supernatants were obtained by centrifugation, and the NO content was detected according to the manufacturer's instructions using an NO assay kit (Nanjing Jiancheng, China). The pulmonary arteries of the mice were sectioned and stained with a DAF-FM DA probe (Beyotime Biotechnology) and incubated at 37 °C for 20 min, and then examined under a microscope.

2.10. Immunohistochemical staining

Pulmonary arteries were sliced, dewaxed and hydrated before staining. Pulmonary artery tissues were sectioned and subjected to antigen retrieval before being incubated with primary antibodies and secondary antibodies were incubated separately to produce visual color reactions using chromogenic agents such as DAB (Beyotime Biotechnology). The sections were restained, dehydrated, and sealed after clearing treatment, and finally observed under the microscope.

2.11. Western blot

Mitochondria were prepared from fresh pulmonary artery tissue and HPAECs. The BCA method was used to measure the protein concentration, and the proteins were separated by SDS–PAGE and transferred to a PVDF membrane. After the membrane was sealed, primary antibodies against TXNIP, TRX, ASC, Caspase-1, PINK, Parkin, P62, Beclin-1, LC3 and β-actin (Proteintech), p-eNOS, eNOS, ICAM-1, VCAM-1, NLRP3, and IL-1β (ABclonal) and secondary antibodies (HRP-conjugated secondary antibodies, Proteintech) were incubated successively. The target proteins were determined using a chemical light emission method, and protein bands were analyzed following exposure and scanning of X-ray photographs.

2.12. Measurement of intercellular ROS and mitoROS

The pulmonary artery tissue was fixed and sectioned or cells were cultured to a suitable state, followed by the probe solution from the Reactive Oxygen Kit (Beyotime Biotechnology) to label the ROS. Pulmonary artery tissues or cultured cells were treated with the ROS probe solution from the Reactive Oxygen Species Assay Kit (Beyotime Biotechnology) according to the manufacturer's instructions.

2.13. Determination of antioxidant enzymes (GSH-px, SOD) and MDA

Sample solutions were prepared from pulmonary artery tissue or cells, mixed with the reaction system and incubated at 37 °C for 20 min according to the kit guidelines to determine absorbance.

2.14. Enzyme-linked immunosorbent assay (ELISA)

Tumor necrosis factor alpha (TNF-α) and interleukin 6 (IL-6) levels in pulmonary artery tissue or cell culture supernatants were measured by ELISA (Mlbio; Shanghai, China).

2.15. Immunofluorescence staining

Fixation, osmotic treatment of pulmonary artery tissues or cells, sequential incubation with primary antibodies and fluorescently labeled secondary antibodies (Beyotime Biotechnology), and finally observation via fluorescence microscopy.

2.16. Cell viability assay

CCK8 reagent was added to the cell culture media, and the change in absorbance was measured by colorimetric assay after incubation for a period of time.

2.17. Mitochondrial membrane potential (ΔΨm) measurement

The JC-1 probe (Beyotime Biotechnology) was added to the cell culture for staining, and then detected by fluorescence microscopy.

2.18. Mitochondrial and lysosomal fluorescence staining

First, the cells were cultured to the appropriate density, and the cells were fixed with 4 % paraformaldehyde, the mitochondria were stained with MitoTracker, while the lysosomes were stained with LysoTracker. After staining, the cells were washed with PBS, and observation via fluorescence microscopy.

2.19. Statistical analysis

All the data are presented as the standard deviation plus or minus the average and were analyzed using GraphPad Prism 8.0 software. Statistical analysis was performed using SPSS 26.0 software, and $P < 0.05$ indicated statistical significance.

3. Results

1. Network Pharmacology Analysis to Explore Rg1 Targets in the Treatment of PAH

A total of 120 targets related to Rg1 were identified from the SEA, ECTM and SwissTarget databases. Moreover, 7144 PAH-related targets and 7792 pulmonary VED-related targets were identified from the OMIM, DisGeNET and GeneCards databases. Using Venn diagrams, we identified 106 common targets of PAH, pulmonary VED and Rg1 were identified (Fig. 1A). To explore the mechanism by which Rg1 treats PAH, 106 common targets were identified via the STRING database, and a protein–protein interaction (PPI) network was constructed. The network contained 104 nodes and 1161 edges, and the median values close to degree centrality (DC), betweenness centrality (BC), and proximity centrality (CC) were 22.33, 101.5, and 0.005, respectively. The core PPI network was identified on the basis of topology analysis, and 12 core targets were identified using the median DC ≥ 44.66 (Fig. 1B). Core and noncore target networks were constructed (Fig. 1C). In the network, the size of the node was proportional to the degree of value. Cluster analysis using MCODE was performed, a highly connected subnetwork was generated, and the targets were assigned to 5 groups (Fig. 1D). The top 20 hub genes according to the molecular combination score (MCC) sequence were screened with the Cytohubba plugin (Fig. 1E). To further explore the mechanisms by which Rg1 promotes PAH treatment, GO enrichment and KEGG pathway analyses of 106 intersecting genes and their biological functions and related pathways were performed.

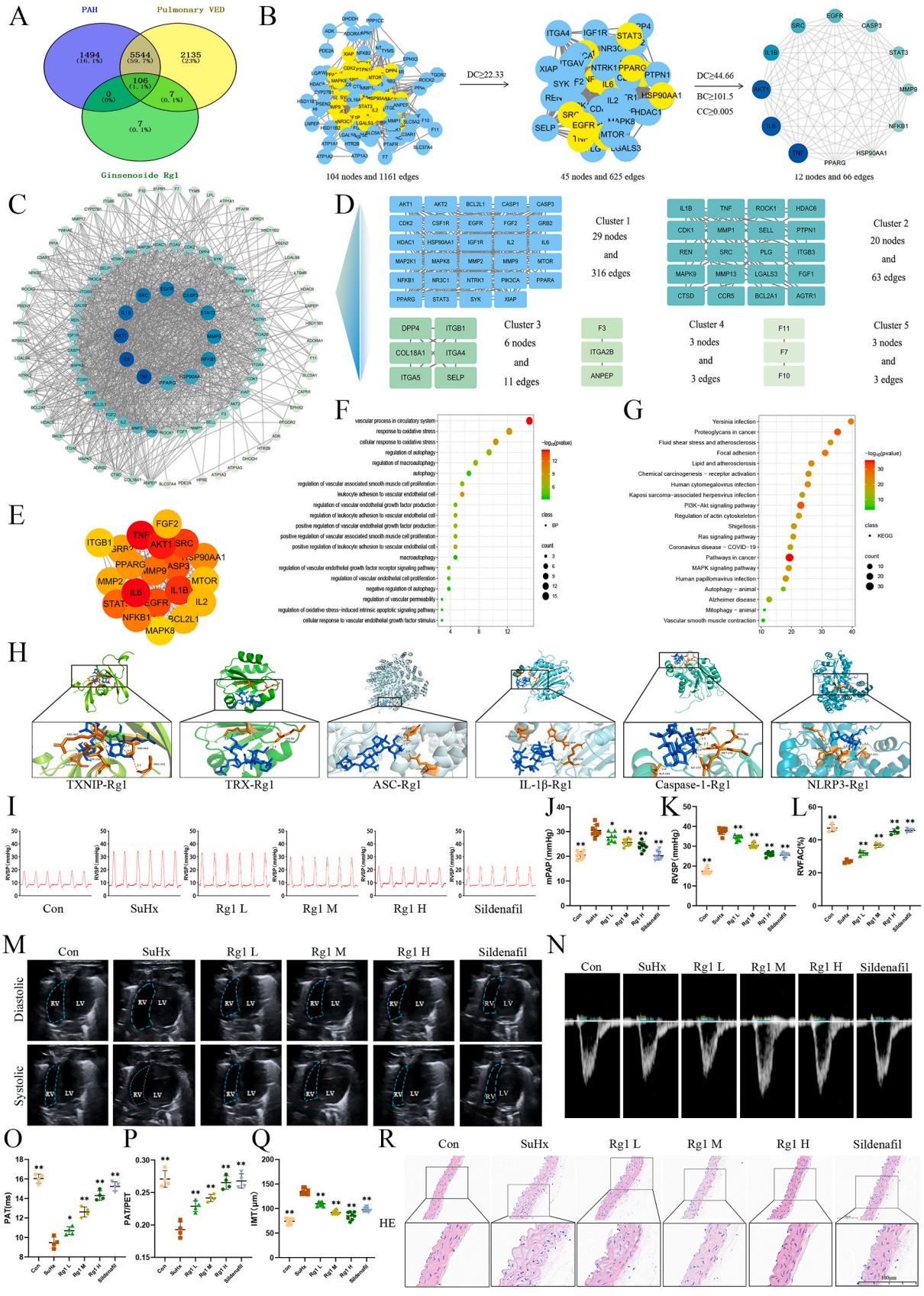

Fig. 1. Network pharmacology analysis to explore Rg1 targets in the treatment of PAH and Rg1 ameliorates hypoxia-induced PAH. (A) Venn diagram. (B) Topology analysis. (C) PPI network. (D) Cluster analysis. (E) Hub genes. (F) Bioprocess category terms from GO enrichment analysis. (G) KEGG analysis. (H) Molecular docking. (I–K) RVSP and mPAP hemodynamic analysis (n = 8). (L, M) Representative B-mode apical four-chamber right ventricular. RVFAC=(right ventricular end diastolic area - right ventricular end systolic area)/right ventricular end diastolic area × 100 %] (n = 4). (N–P) Ultrasonic heart map of pulmonary blood flow (n = 4). (Q, R) H&E staining images (n = 8). **P < 0.01, *P < 0.05 compared to the SuHx group.

Notably, Rg1 was found to be involved in many biological processes, especially the oxidative stress response, regulation of autophagy, and vascular-related regulation (Fig. 1F). KEGG pathway analysis revealed that Rg1 was significantly associated with vascular smooth muscle contraction, mitophagy-animal, and autophagy-animal (Fig. 1G). According to past research, the TXNIP/NLRP3 signaling pathway is closely related to oxidative stress and inflammatory reactions [11–13]. Based our network pharmacology study, we revealed that the TXNIP/NLRP3 signaling pathway may be a potential target for treating PAH and further explored the potential effect and mechanism of Rg1 on PAH. Molecular docking analysis of TXNIP/NLRP3 proteins involved in signaling pathways and Rg1 was used to examine the interaction between the protein

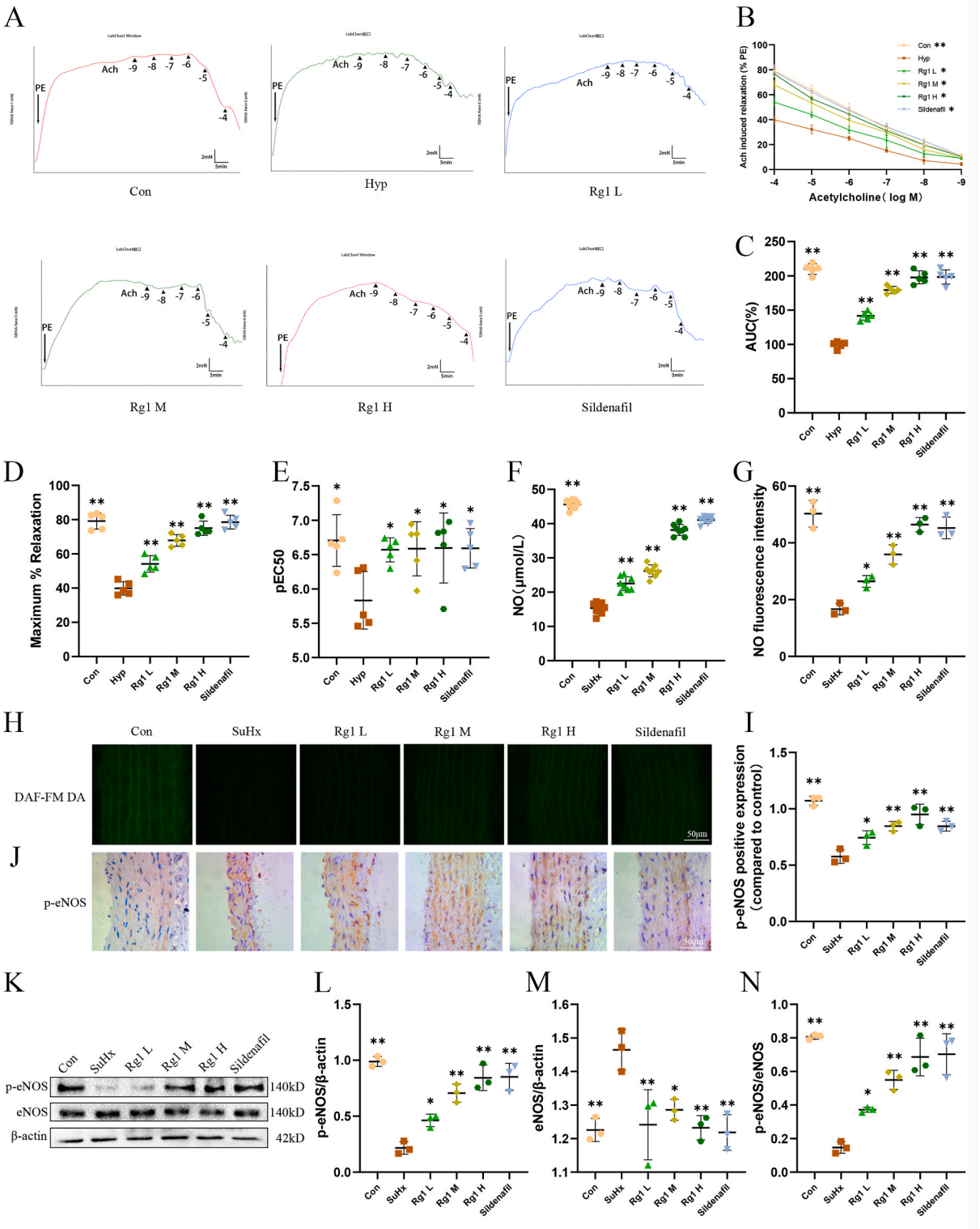

Fig. 2. Rg1 alleviates VED in SuHx Mice. (A–E) Endothelium-dependent vasodilation reaction (n = 5). (F–H) NO level (n = 8) and DAF-FM DA fluorescence image (n = 3). (I–J) Immunohistochemical detection of p-eNOS expression (n = 3). (K–N) P-eNOS and eNOS protein expression (n = 3). **P < 0.01, *P < 0.05 compared to the SuHx group.

and Rg1 affinity, and the results showed strong binding between pathway-related proteins and Rg1 (Fig. 1H).

2. Rg1 Ameliorates Hypoxia-induced PAH

This study investigated the possible therapeutic effect of Rg1 on PAH utilizing a mouse model of PAH induced by hypoxia combined with su5416. Hemodynamics tests revealed that the mPAP of SuHx mice increased markedly four weeks after hypoxia. In the SuHx group, the mPAP was significantly greater than that in the Con group. Compared with the SuHx group, the application of Rg1 at different doses and Sildenafil reduced the mPAP of SuHx mice to varying degrees (Fig. 1K). PAH is known to impose excessive pressure on the right ventricle, making the assessment of RVSP essential. The present study showed that RVSP was significantly greater in SuHx mice than in Con mice. Compared with SuHx, different doses of Rg1 and Sildenafil decreased RVSP in SuHx mice (Fig. 1I and J). Echocardiographic analysis revealed a significant reduction in PAT and PAT/PET in the SuHx group. However, treatment with different doses of Rg1 and Sildenafil ameliorated these changes (Fig. 1N-P). B-mode echocardiography revealed an increase in RV hypertrophy and RV area in the SuHx group compared to the Con group (Fig. 1L and M). Treatment with varying doses of Rg1 and Sildenafil resulted in varying degrees of improvement in the RVFAC. The Con group exhibited thin pulmonary vessel walls with a uniform cellular distribution and an absence of significant perivascular inflammatory cell infiltration. In contrast, the SuHx group exhibited marked thickening of the pulmonary vascular walls and endometrium, disorganized endothelial cell arrangement, and marked inflammatory cell infiltration. Treatment with different doses of Rg1 and Sildenafil improved pulmonary vascular tissue pathology in SuHx mice (Fig. 1Q and R).

3. Rg1 Alleviates VED in SuHx Mice

VED is characterized by a reduced vasodilatory response and reduced production of NO and eNOS. In this study, we observed that ach-induced pulmonary artery vasodilatory function was impaired in Hyp mice compared with Con mice. Different doses of Rg1 and Sildenafil partially reversed these changes (Fig. 2A–E). The pulmonary artery NO concentration in the SuHx group was lower than that in the Con group. Treatment with different doses of Rg1 and Sildenafil partially reversed this reduction (Fig. 2F–H). Immunohistochemical and Western blot analyses revealed that the pulmonary arteries of SuHx mice had reduced numbers of p-eNOS-positive cells and p-eNOS and eNOS protein levels, and these effects were reversed by different doses of Rg1 and Sildenafil (Fig. 2I-N).

4. Rg1 Alleviates Oxidative Stress, Inflammation and Mitophagy in SuHx Mice

Compared to the Con group, the SuHx group exhibited increased levels of MDA, intracellular ROS, and mitoROS and decreased SOD activity and GSH-px levels. Notably, treatment with Rg1 at various doses and Sildenafil partially reversed these alterations to varying degrees (Fig. 3A–G). Compared to those in the Con group, the levels of TNF-α and IL-6 were significantly elevated in the pulmonary arteries of SuHx mice, and the protein expression of ICAM-1 and VCAM-1 was significantly elevated. Treatment with different doses of Rg1 and Sildenafil reversed these changes to varying degrees (Fig. 3H-L). Western blot analysis revealed that the expression levels of PINK1, Parkin, Beclin-1 and LC3-II in the pulmonary arteries of SuHx mice were increased compared with those in the Con group. Meanwhile, the expression levels of p62 decreased. Treatment with different doses of Rg1 and Sildenafil reversed these mitophagy-related changes compared with those in the SuHx group (Fig. 3M − P).

5. Impact of Rg1 on the TXNIP/NLRP3 Pathway

The ratio of TXNIP- and NLRP3-positive cells in the pulmonary arteries of the SuHx group mice increased markedly compared to that in the Con group. However, different doses of Rg1 and Sildenafil reversed these changes to varying degrees (Fig. 4A–C). In SuHx mice, the pulmonary artery TXNIP protein level was increased, the TRX level was decreased, and the expression of the NLRP3 inflammatory small components NLRP3, ASC, IL-1β and Caspase-1 were high. Rg1 and Sildenafil alleviated these changes in a dose-dependent manner (Fig. 4D–J).

6. Impact of Rg1 on the TXNIP/NLRP3 Pathway and Mitophagy in Hypoxia-Induced VED

In this study we investigated the role of Rg1 in the TXNIP/NLRP3 pathway in hypoxia-induced VED using an in vitro culture method. Pulmonary arteries were obtained from normal mice and treated with SRI37330 (a TXNIP inhibitor) or MCC950 (an NLRP3 inhibitor) for 24 h under hypoxic conditions for vasodilation response assays. Both SRI37330 and MCC950 improved the ach-induced pulmonary vasodilatory response under hypoxic conditions compared with that in the Hyp group. Similarly, treatment with Rg1 and Sildenafil improved the pulmonary vasodilatory response to varying degrees (Fig. 4K, L and N-P). To explore the role of mitophagy in hypoxia-induced VED, pulmonary arteries from normal mice were incubated with Rg1 + SB203580 (a mitophagy agonist) and Liensinine (a mitophagy inhibitor) for 24 h under hypoxic conditions for vasodilation response assays. When compared with Hyp, Rg1 and Sildenafil improved the Ach-induced pulmonary vasodilatory response under hypoxic conditions, similar to the effect of Liensinine. Additionally, SB203580 was used to eliminate the protective effects of Rg1 (Fig. 4K, M and Q-S).

7. Rg1 Alleviates Endothelial Dysfunction via the TXNIP/NLRP3 Pathway in Hypoxia-Induced HPAECs

The optimal drug concentration for subsequent experiments was determined by assessing the viability of HPAECs treated with different concentrations of Rg1 under hypoxic conditions. Rg1 at a dose of 5 μM and 10 μM did not significantly affect cell viability compared to that in the Hyp group. Increased doses resulted in a marked improvement, with significant effects observed at 20 μM, 40 μM, and 80 μM. Therefore, 20 μM was selected as the optimal concentration for subsequent experiments (Fig. 5A). Next, comparison of cell viability among the different drug groups revealed that compared with Hyp, SRI37330, MCC950, Rg1, and Sildenafil increased cell viability (Fig. 5B). Compared to those in the Con group, hypoxia-induced HPAECs exhibited decreased NO production and p-eNOS expression. Treatment with SRI37330, MCC950, Rg1, or Sildenafil partially reversed these effects to varying degrees (Fig. 5C–K).

8. Rg1 Ameliorates Oxidative Stress and Inflammation via the TXNIP/NLRP3 Pathway in Hypoxia-Induced HPAECs

Compared to those in the Con group, the Hyp group MitoROS, intracellular ROS and MDA levels increased, and SOD and GSH-px levels decreased. Similar to the effects on endothelial function, treatment with SRI37330, MCC950, Rg1 and Sildenafil partially reversed these alterations (Fig. 5L-R). The Hyp group exhibited increased levels of TNF-α and IL-6 and elevated ICAM-1 and VCAM-1 protein expression. Treatments of SRI37330, MCC950, Rg1 and Sildenafil similarly reversed these inflammation-related changes (Fig. 5S-W).

9. Impact of Rg1 on the TXNIP/NLRP3 Pathway in Hypoxia-Induced HPAECs

In the Hyp group, the TXNIP protein level was increased, the TRX level was decreased, and the expression of the NLRP3 inflammatory small components NLRP3, ASC, IL-1β and Caspase-1 were high.

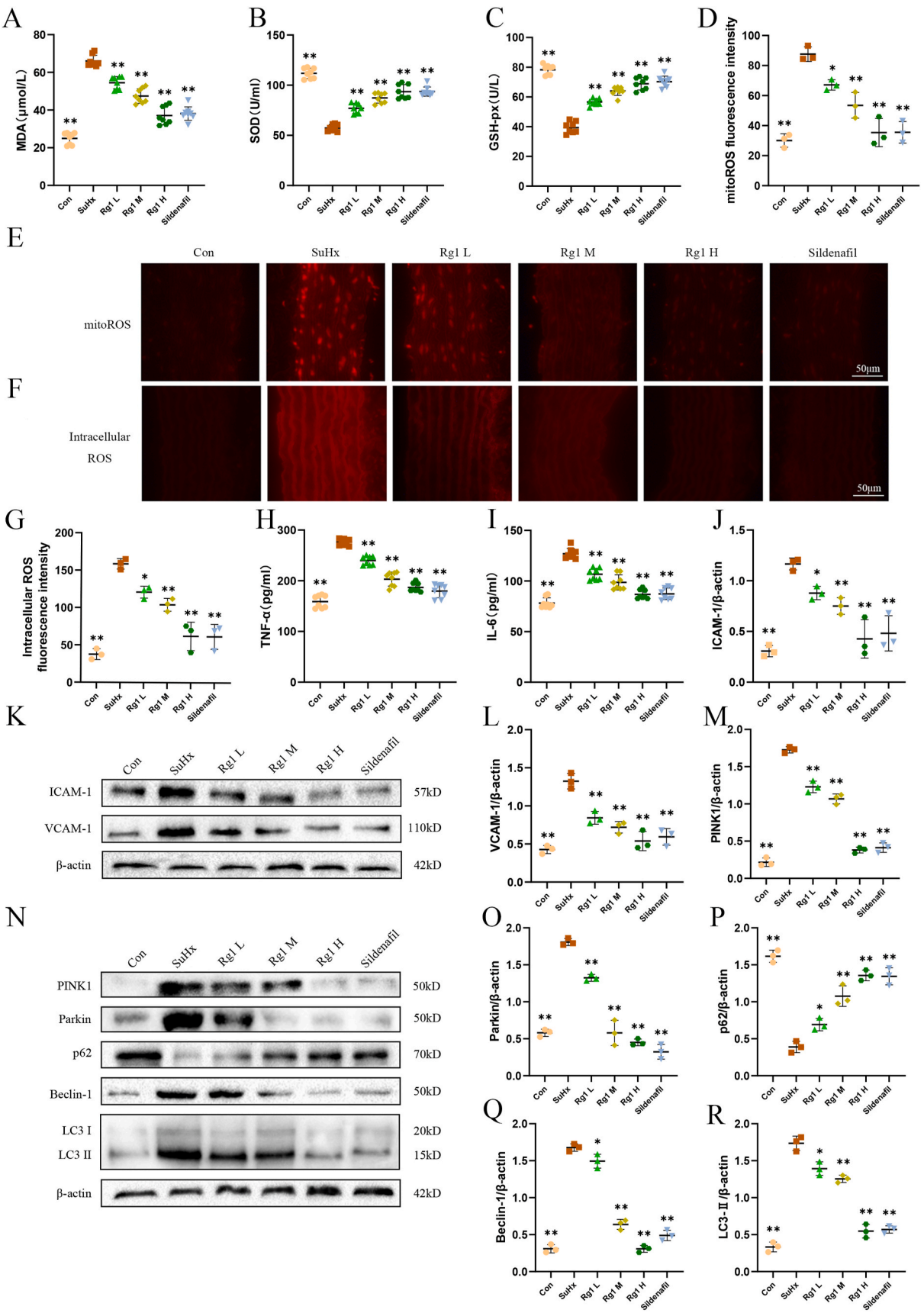

Fig. 3. Rg1 alleviates oxidative stress, inflammation and mitophagy in SuHx mice. (A–C) SOD activity, MDA and GSH -PX levels (n = 8). (D–G) Fluorescence of MitoROS and intracellular ROS (n = 3). (H and I) TNF-α and IL-1βlevels (n = 8). (J–L) ICAM-1 and VCAM-1 protein expression (n = 3). (M–R) PINK1, Parkin, p62, Beclin-1, and LC3-II protein expression (n = 3). **P < 0.01, *P < 0.05 compared to the SuHx group.

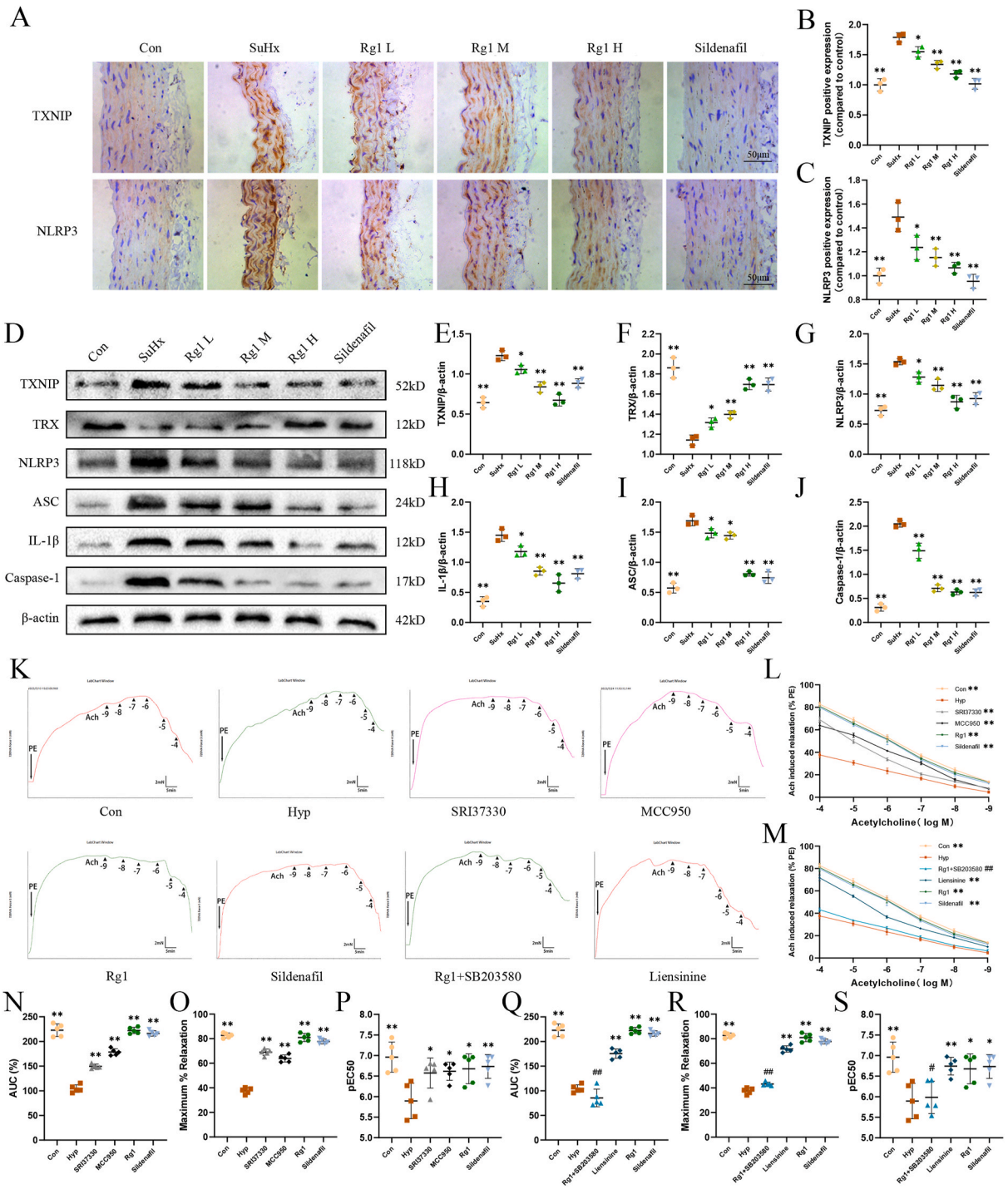

Fig. 4. Impact of Rg1 on the TXNIP/NLRP3 pathway and mitophagy in hypoxia-induced VED. (A–C) Immunohistochemical detection of TXNIP and NLRP3 expression (n = 3). (D–J) TXNIP, TRX, NLRP3, ASC, IL-1β and Caspase-1 protein expression (n = 3). (K,L and N-P) Rg1 impact on TXNIP/NLRP3 pathway in hypoxia-induced VED (n = 5). (K, M and Q-S) Effect of Rg1 on mitophagy in hypoxia-induced VED (n = 5). *P < 0.05, **P < 0.01 compared to the Hyp group. $^{\#}$P < 0.05, $^{\#\#}$P < 0.01 compared to the Rg1 group.

Treatment with SRI37330, MCC950, Rg1, or Sildenafil reversed these changes (Fig. 6A–J).

10. Rg1 Ameliorates Mitophagy via the TXNIP/NLRP3 Pathway in Hypoxia-Induced HPAECs

In this study, SRI37330, MCC950, Rg1, and Sildenafil increased cell viability and Δψm and p62 protein expression in hypoxia-induced HPAECs. In addition, PINK1, Parkin, Beclin-1, and LC3-II protein expression and mitophagy levels were reduced, and these effects were similar to those of Liensinine. When SB203580 was combined with Rg1, the protective effect of Rg 1 was disrupted, leading to similar results as the Hyp group (Fig. 6K-U).

4. Discussion

In this study, we explored the therapeutic mechanism of Rg1 in PAH using network pharmacology. First, targets related to PAH, pulmonary

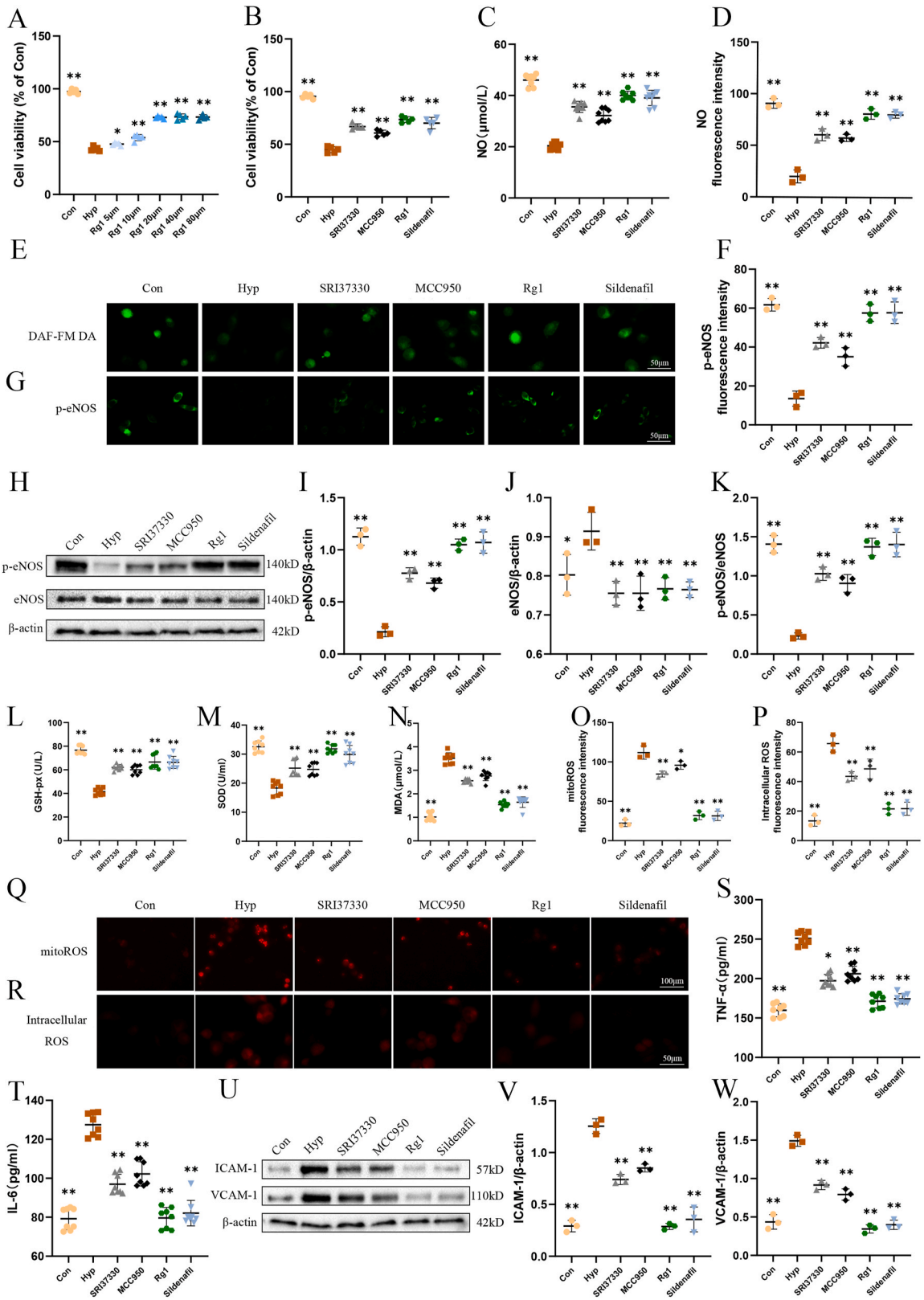

Fig. 5. Rg1 alleviates endothelial dysfunction, oxidative stress and inflammation via the TXNIP/NLRP3 pathway in hypoxia-induced HPAECs. (A) Cell viability at different drug concentrations (n = 5). (B) Cell activity of different groups (n = 5). (C–E) NO levels (n = 8) and DAF-FM DA fluorescence (n = 3). (G–F) Immunohistochemical detection of p-eNOS expression (n = 3). (H–K) P-eNOS and eNOS protein expression (n = 3). (L–N) SOD activity, MDA and GSH-px levels (n = 8). (O–R) MitoROS and intracellular ROS fluorescence (n = 3). (S and T) TNF-α and IL-6 levels (n = 8). (U–W) ICAM-1 and VCAM-1 protein expression (n = 3). *P < 0.05, **P < 0.01 compared to the Hyp group.

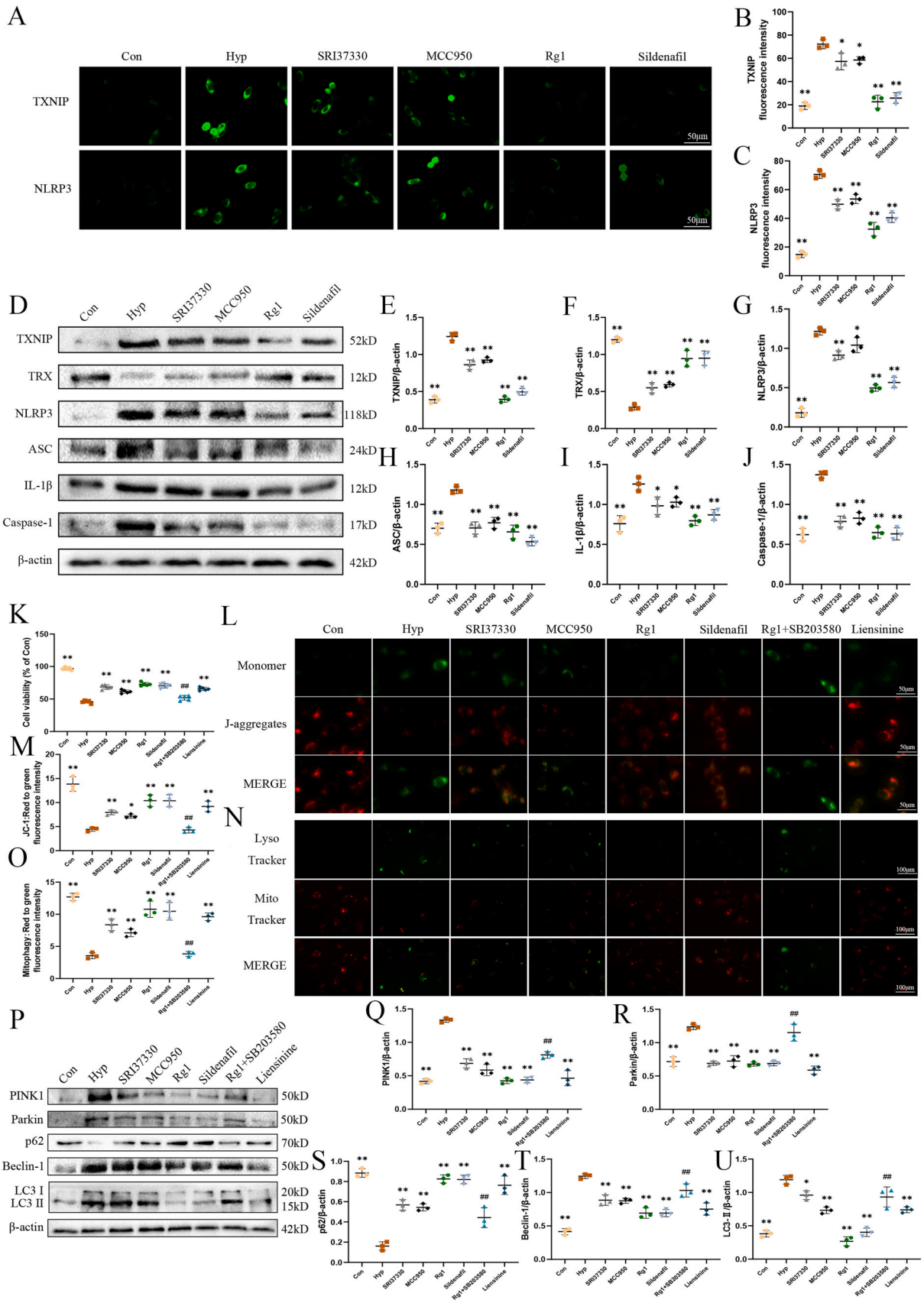

Fig. 6. Rg1 ameliorates mitophagy via the TXNIP/NLRP3 pathway in hypoxia-induced HPAECs. (A–C) TXNIP, NLRP3 fluorescence (n = 3). (D–J) TXNIP, TRX, NLRP3, ASC, IL-1β and Caspase-1 protein expression (n = 3). (K) Cell activity of different groups (n = 5). (L,M) ΔΨm (n = 3). (N,O) Lyso-Tracker Green and Mito-Tracker Red CMXRos staining (n = 3). (P–U) Pink 1, Parkin, p62, Beclin-1, LC3 protein expression (n = 3). *P < 0.05, **P < 0.01 compared to the Hyp group. $^{\#}$P < 0.05, $^{\#\#}$P < 0.01 compared to the Rg1 group.

VED and Rg1 were identified from different databases, and 106 common targets were identified via a Venn diagram. The STRING database was used to construct the PPI network, and topological features were used to screen 12 core targets. In addition, the MCODE algorithm was used to distinguish between core and noncore targets, and subsequent cluster analysis of highly connected subnetworks was performed. GO enrichment and KEGG pathway analyses revealed multifaceted roles of Rg1 in the oxidative stress response, autophagy regulation, and vascular regulation. The significant association of Rg1 with pathways such as vascular smooth muscle contraction and mitophagy underscores its potential therapeutic role in PAH. The TXNIP/NLRP3 pathways are involved in oxidative stress and inflammation. Further molecular docking analysis showed that Rg1 had strong binding activity with proteins related to this pathway, which suggests that Rg1 may be a potential target for the treatment of PAH. Our study provided a comprehensive network pharmacology analysis, and based on these results, we performed further experimental validation.

PAH is characterized by progressive pulmonary vascular resistance, increased right ventricular load, and vascular remodeling, and VED plays a pivotal role in its pathogenesis [25]. Our findings align with recent studies that underscore the role of VED in PAH [26,27]. Previous research from our laboratory confirmed the protective effects of Rg1 against VED induced by chronic intermittent hypoxia and hyperglycemia [20,21]. However, the precise mechanisms of Rg1 in PAH-related VED are still under investigation. The present study demonstrated that Rg1 intervention was effective in reducing pulmonary arterial pressure, improving morphological changes in the pulmonary vasculature, enhancing endothelium-dependent vasodilation, and maintaining the vascular steady state. This study revealed that Rg1 enhanced the expression of NO and eNOS and improved endothelium-dependent vasodilatation, thereby attenuating the onset and progression of VED.

VED in PAH is primarily driven by oxidative stress, leading to endothelial cell damage and inflammation [28–31]. Our study suggests that Rg1 treatment increases antioxidant defenses such as SOD and GSH-Px activity and decreases the levels of MDA and proinflammatory cytokines such as TNF-α and IL-6. The protective effect of Rg1 against hypoxia-induced VED was demonstrated by improved endothelium-dependent vasodilatation, reduced oxidative stress and inflammatory responses, which is a greater advance than studies focusing primarily on the effects of conventional vasodilators [32].

Mitochondrial dysfunction is closely associated with oxidative stress and inflammation in VED [33,34]. In addition, activation of mitophagy under hypoxic conditions is associated with the clearance of damaged mitochondria, thereby reducing ROS production and subsequent inflammatory responses [35]. These results indicate that Rg1 decreased the expression levels of the mitophagy markers, suggesting a decrease in hypoxia-induced mitophagy. In vitro vascular tension measurements of pulmonary arteries from normal mice using SB203580 and Liensinine revealed that the effects of Rg1 are similar to those of Liensinine and that the addition of SB203580 to Rg1 abolishes its protective effects. Recent studies have emphasized the importance of mitochondrial quality in controlling endothelial cell function and survival [36], which is supported by our findings that Rg1 reduces mitochondrial membrane potential and mitophagy activation in hypoxia-induced HPAECs.

TXNIP interacts with multiple proteins, and is associated with various diseases [37–39]. Oxidative stress and inflammation are well-recognized drivers of VED, and the TXNIP/NLRP3 pathway plays a central role in the inflammatory response to cellular stressors [40,41]. Previous studies have demonstrated that hypoxia-induced mitochondrial dysfunction triggers the TXNIP/NLRP3 pathway, leading to endothelial cell damage [42]. The TXNIP/NLRP3 axis is associated with the inflammatory response and endothelial cell injury in PAH [43,44], and modulation of the TXNIP/NLRP3 pathway can alleviate VED [45]. Our study revealed that Rg1, similar to SRI37330 and MCC950, improves hypoxia-induced endothelium-dependent vasodilation and reduces the vitality of HPAECs by decreasing TXNIP levels, increasing TRX levels, down-regulating NLRP3 inflammasome components, modulating inflammation and oxidative stress. These results suggest that Rg1 may exert its protective effects through the TXNIP/NLRP3 pathway. Consistent with our observation that Rg1 regulates this pathway and alleviates oxidative stress [46].

The protective effect of Rg1 observed in our study is particularly interesting due to limited therapeutic options for PAH. Current treatments often do not address endothelial dysfunction. According to a previous study, Rg1 improves hypoxia-induced pulmonary revascularization in PAH and hypoxia hypercapnia-induced vasoconstriction [47,48]. Our study suggests that Rg1, similar to SRI37330, MCC950, and Liensinine, improves endothelium-dependent vasodilation and HPAEC viability under hypoxic conditions by modulating oxidative stress, inflammation, and mitophagy, highlighting its protective role against hypoxia-induced VED. This indicates that Rg1 may modulate mitophagy through the TXNIP/NLRP3 pathway to exert its protective effects, providing a novel therapeutic strategy for PAH [49].

In summary our study provides evidence that Rg1 improves endothelial dysfunction in PAH by reducing oxidative stress, inflammation, and mitophagy and that its protective effect is mediated through the TXNIP/NLRP3 pathway, suggesting that Rg1 may be a potential agent for PAH treatment.

Acknowledgments

This study was supported by the National Natural Science Foundation of China (No. 82474170).

References

[1] Burton Vj, Li Ciuclan, Holmes Am, Dm Rodman, Walker C, Budd Dc. Bone morphogenetic protein receptor II regulates pulmonary artery endothelial cell barrier function. Blood 2011;117:333–41.
[2] Evans Ce, Cober Nd, Dai Z, Stewart Dj, Yy Zhao. Endothelial cells in the pathogenesis of pulmonary arterial hypertension. Eur Respir J 2021;58.
[3] Wu Y, Pan B, Zhang Z, Li X, Leng Y, Ji Y, Sun K, Chen Af. Caspase-4/11-Mediated pulmonary artery endothelial cell pyroptosis contributes to pulmonary arterial hypertension. HYPERTENSION 2022;79:536–48.
[4] de Jesus Perezva, Alastalo Tp, Wu Jc, Axelrod Jd, Cooke Jp, Amieva M, Rabinovitch M. Bone morphogenetic protein 2 induces pulmonary angiogenesis via Wnt-beta-catenin and Wnt-RhoA-Rac1 pathways. J Cell Biol 2009;184:83–99.
[5] Aimaier S, Tao Y, Lei F, Yupeng Z, Wenhui S, Aikemu A, Maimaitiyiming D. Protective effects of the Terminalia bellirica tannin-induced Nrf2/HO-1 signaling pathway in rats with high-altitude pulmonary hypertension. BMC Complement Med Ther 2023;23:150.
[6] Csiszar A, Labinskyy N, Olson S, Pinto Jt, Gupte S, Wu Jm, Hu F, Ballabh P, Podlutsky A, Losonczy G, et al. Resveratrol prevents monocrotaline-induced pulmonary hypertension in rats. HYPERTENSION 2009;54:668–75.
[7] Hudson J, Farkas L. Epigenetic regulation of endothelial dysfunction and inflammation in pulmonary arterial hypertension. Int J Mol Sci 2021;22.
[8] Cloonan Sm, Choi Am. Mitochondria in lung disease. J Clin Invest 2016;126:809–20.
[9] Culley Mk, Chan Sy. Mitochondrial metabolism in pulmonary hypertension: beyond mountains there are mountains. J Clin Invest 2018;128:3704–15.
[10] Singh N, Manhas A, Kaur G, Jagavelu K, Hanif K. Inhibition of fatty acid synthase is protective in pulmonary hypertension. Br J Pharmacol 2016;173:2030–45.
[11] Devi Ts, Lee I, Hüttemann M, Kumar A, Nantwi Kd, Singh Lp. TXNIP links innate host defense mechanisms to oxidative stress and inflammation in retinal Muller glia under chronic hyperglycemia: implications for diabetic retinopathy. Exp Diabetes Res 2012;2012:438238.
[12] Yoshihara E, Masaki S, Matsuo Y, Chen Z, Tian H, Yodoi J. Thioredoxin/Txnip: redoxisome, as a redox switch for the pathogenesis of diseases. Front Immunol 2014;4:514.
[13] Bai B, Yang Y, Wang Q, Li M, Tian C, Liu Y, Aung Lhh, Li Pf, Yu T, Chu Xm. NLRP3 inflammasome in endothelial dysfunction. Cell Death Dis 2020;11:776.
[14] Zhou R, Yazdi As, Menu P, Tschopp J. A role for mitochondria in NLRP3 inflammasome activation. NATURE 2011;469:221–5.
[15] Han Y, Li X, Yang L, Zhang D, Li L, Dong X, Li Y, Qun S, Li W. Ginsenoside Rg1 attenuates cerebral ischemia-reperfusion injury due to inhibition of NOX2-mediated calcium homeostasis dysregulation in mice. J GINSENG RES 2022;46:515–25.
[16] He C, Feng R, Sun Y, Chu S, Chen J, Ma C, Fu J, Zhao Z, Huang M, Shou J, et al. Simultaneous quantification of ginsenoside Rg1 and its metabolites by HPLC-MS/MS: rg1 excretion in rat bile, urine and feces. Acta Pharm Sin B 2016;6:593–9.
[17] Ji P, Shi Q, Liu Y, Han M, Su Y, Sun R, Zhou H, Li W, Li W. Ginsenoside Rg1 treatment alleviates renal fibrosis by inhibiting the NOX4-MAPK pathway in T2DM mice. Ren Fail 2023;45:2197075.

[18] Zhang L, Li Y, Ma X, Liu J, Wang X, Zhang L, Li C, Li Y, Yang W. Ginsenoside Rg1-Notoginsenoside R1-Protocatechuic aldehyde reduces atherosclerosis and attenuates Low-Shear Stress-Induced vascular endothelial cell dysfunction. Front Pharmacol 2020;11:588259.
[19] Zhu T, Wang H, Wang L, Zhong X, Huang W, Deng X, Guo H, Xiong J, Xu Y, Fan J. Ginsenoside Rg1 attenuates high glucose-induced endothelial barrier dysfunction in human umbilical vein endothelial cells by protecting the endothelial glycocalyx. Exp Ther Med 2019;17:3727–33.
[20] Lu M, Zhao F, Ran C, Xu Y, Zhang J, Wang H. Ginsenoside Rg1 attenuates diabetic vascular endothelial dysfunction by inhibiting the calpain-1/ROS/PKC-β axis. Life Sci 2023;329:121972.
[21] Zhao F, Lu M, Wang H. Ginsenoside Rg1 ameliorates chronic intermittent hypoxia-induced vascular endothelial dysfunction by suppressing the formation of mitochondrial reactive oxygen species through the calpain-1 pathway. J GINSENG RES 2023;47:144–54.
[22] Ni Wang, Yang Junyan, Chen Ruijun, Liu Yunyun, Liu Shunjie, Pan Yining, Lei Qingfeng, Wang Yuzhou, He Lu, Song Youqiang, et al. Ginsenoside Rg1 ameliorates Alzheimer's disease pathology via restoring mitophagy. J GINSENG RES 2023;47:448–57.
[23] Guan S, Xin Y, Ding Y, Zhang Q, Han W. Ginsenoside Rg1 protects against cardiac remodeling in heart failure via SIRT1/PINK1/parkin-mediated mitophagy. Chem Biodivers 2023;20:e202200730.
[24] Lin J, Qing Z, Huang H, Yang S, Zeng Z. Ginsenoside rg1 alleviates rat liver Ischemia-Reperfusion ischemia through mitochondrial autophagy pathway. Altern Ther Health Med 2023;29:16–25.
[25] Weatherald J, Boucly A, Peters A, Montani D, Prasad K, Psotka Ma, Zannad F, Gomberg-Maitland M, McLaughlin V, Simonneau G, et al. The evolving landscape of pulmonary arterial hypertension clinical trials. LANCET (N AM ED) 2022;400:1884–98.
[26] Wang R, Guo Y, Li L, Luo M, Peng L, Lv D, Cheng Z, Xue Q, Wang L, Huang J. Role of thioredoxin-interacting protein in mediating endothelial dysfunction in hypertension. Genes Dis 2022;9:753–65.
[27] Zhang Y, Xing Cj, Liu X, Li Yh, Jia J, Feng Jg, Yang Cj, Chen Y, Zhou J. Thioredoxin-Interacting protein (TXNIP) knockdown protects against Sepsis-Induced brain injury and cognitive decline in mice by suppressing oxidative stress and neuroinflammation. Oxid Med Cell Longev 2022;2022:8645714.
[28] El Alams, Pena E, Aguilera D, Siques P, Brito J. Inflammation in pulmonary hypertension and edema induced by hypobaric hypoxia exposure. Int J Mol Sci 2022;23.
[29] Klein F, Dinesh S, Fiedler D, Grün K, Schrepper A, Bogoviku J, Bäz L, Pfeil A, Kretzschmar D, Schulze Pc, et al. Identification of serum interleukin-22 as novel biomarker in pulmonary hypertension: a translational study. Int J Mol Sci 2024;25.
[30] Ozaki E, Campbell M, Doyle Sl. Targeting the NLRP3 inflammasome in chronic inflammatory diseases: current perspectives. J Inflamm Res 2015;8:15–27.
[31] Rabinovitch M, Guignabert C, Humbert M, Nicolls Mr. Inflammation and immunity in the pathogenesis of pulmonary arterial hypertension. Circ Res 2014;115:165–75.
[32] Yang M, Linn Bs, Zhang Y, Ren J. Mitophagy and mitochondrial integrity in cardiac ischemia-reperfusion injury. Biochim Biophys Acta, Mol Basis Dis 2019;1865:2293–302.
[33] Feng W, Wang J, Yan X, Zhang Q, Chai L, Wang Q, Shi W, Chen Y, Liu J, Qu Z, et al. ERK/Drp1-dependent mitochondrial fission contributes to HMGB1-induced autophagy in pulmonary arterial hypertension. Cell Prolif 2021;54:e13048.
[34] Gomez-Puerto Mc, van Zuijen I, Huang Cj, Szulcek R, Pan X, van Dinther Ma, Kurakula K, Wiesmeijer Cc, Goumans Mj, Bogaard Hj, et al. Autophagy contributes to BMP type 2 receptor degradation and development of pulmonary arterial hypertension. J Pathol 2019;249:356–67.
[35] Chen W, Zhao H, Li Y. Mitochondrial dynamics in health and disease: mechanisms and potential targets. Signal Transduct Target Ther 2023;8:333.
[36] Galiè N, Humbert M, Vachiery Jl, Gibbs S, Lang I, Torbicki A, Simonneau G, Peacock A, Vonk Noordegraafa, Beghetti M, et al. [2015 ESC/ERS Guidelines for the diagnosis and treatment of pulmonary hypertension]. Kardiol Pol 2015;73:1127–206.
[37] Han Y, Xu X, Tang C, Gao P, Chen X, Xiong X, Yang M, Yang S, Zhu X, Yuan S, et al. Reactive oxygen species promote tubular injury in diabetic nephropathy: the role of the mitochondrial ros-txnip-nlrp3 biological axis. Redox Biol 2018;16:32–46.
[38] Pan M, Zhang F, Qu K, Liu C, Zhang J. TXNIP: a Double-Edged sword in disease and therapeutic outlook. Oxid Med Cell Longev 2022;2022:7805115.
[39] Woo Sh, Kyung D, Lee Sh, Park Ks, Kim M, Kim K, Kwon Hj, Won Ys, Choi I, Park Yj, et al. TXNIP suppresses the osteochondrogenic switch of vascular smooth muscle cells in atherosclerosis. Circ Res 2023;132:52–71.
[40] Kelley N, Jeltema D, Duan Y, He Y. The NLRP3 inflammasome: an overview of mechanisms of activation and regulation. Int J Mol Sci 2019;20.
[41] Lamkanfi M, Vm Dixit. Inflammasomes and their roles in health and disease. Annu Rev Cell Dev Biol 2012;28:137–61.
[42] Yan Yr, Zhang L, Lin Yn, Sun Xw, Ding Yj, Li N, Li Hp, Li Sq, Zhou Jp, Li Qy. Chronic intermittent hypoxia-induced mitochondrial dysfunction mediates endothelial injury via the TXNIP/NLRP3/IL-1β signaling pathway. Free Radic Biol Med 2021;165:401–10.
[43] Beshay S, Sahay S, Humbert M. Evaluation and management of pulmonary arterial hypertension. Respir Med 2020;171:106099.
[44] Förstermann U, Sessa Wc. Nitric oxide synthases: regulation and function. Eur Heart J 2012;33:829–37. 837a.
[45] Wu Y, Jiang T, Hua J, Xiong Z, Dai K, Chen H, Li L, Peng J, Peng X, Zheng Z, et al. PINK1/Parkin-mediated mitophagy in cardiovascular disease: from pathogenesis to novel therapy. Int J Cardiol 2022;361:61–9.
[46] Sabouny R, Te Shutt. Reciprocal regulation of mitochondrial fission and fusion. TRENDS BIOCHEM SCI 2020;45:564–77.
[47] Tang Bl, Liu Y, Zhang Jl, Lu Ml, Wang Hx. Ginsenoside Rg1 ameliorates hypoxia-induced pulmonary arterial hypertension by inhibiting endothelial-to-mesenchymal transition and inflammation by regulating CCN1. Biomed Pharmacother 2023;164:114920.
[48] Zheng M, Zhao M, Tang L, Zhang C, Song L, Wang W. Ginsenoside Rg1 attenuates hypoxia and hypercapnia-induced vasoconstriction in isolated rat pulmonary arterial rings by reducing the expression of p38. J Thorac Dis 2016;8:1513–23.
[49] Xie Ll, Shi F, Tan Z, Li Y, Bode Am, Cao Y. Mitochondrial network structure homeostasis and cell death. Cancer Sci 2018;109:3686–94.